Available online at www.sciencedirect.com
ScienceDirect
Trans. Nonferrous Met. Soc. China 26(2016) 1791−1800
Transactions of Nonferrous Metals Society of China
www.tnmsc.cn

Microstructure and mechanical properties characterization of AA6061/TiC aluminum matrix composites synthesized by in situ reaction of silicon carbide and potassium fluotitanate

K. JESHURUN LIJAY[1], J. DAVID RAJA SELVAM[2], I. DINAHARAN[3], S. J. VIJAY[2]

1. School of Mechanical Sciences, Karunya University, Coimbatore 641114, Tamil Nadu, India;
2. Center for Research in Metallurgy, School of Mechanical Sciences, Karunya University, Coimbatore 641114, Tamil Nadu, India;
3. Department of Mechanical Engineering Science, University of Johannesburg, Auckland Park Kingsway Campus, Johannesburg 2006, South Africa

Received 27 July 2015; accepted 20 November 2015

Abstract: Aluminum alloys AA6061 reinforced with various amounts (0, 2.5% and 5%, mass fraction) of TiC particles were synthesized by the in situ reaction of inorganic salt K_2TiF_6 and ceramic particle SiC with molten aluminum. The casting was carried out at an elevated temperature and held for a longer duration to decompose SiC to release carbon atoms. X-ray diffraction patterns of the prepared AMCs clearly revealed the formation of TiC particles without the occurrence of any other intermetallic compounds. The microstructure of the prepared AA6061/TiC AMCs was studied using field emission scanning electron microscope (FESEM) and electron backscatter diffraction (EBSD). The in situ formed TiC particles were characterized with homogeneous distribution, clear interface, good bonding and various shapes such as cubic, spherical and hexagonal. EBSD maps showed the grain refinement action of TiC particles on the produced composites. The formation of TiC particles boosted the microhardness and ultimate tensile strength (UTS) of the AMCs.

Key words: aluminum matrix composite; titanium carbide; electron backscatter diffraction; casting; microstructure; mechanical properties

1 Introduction

Aluminium metal matrix composites (AMCs) were developed out of the continuous requirement for lighter weight and higher performance components in aerospace, aircraft and automotive industries. Conventional aluminum alloys are gradually substituted by AMCs in various applications because of superior properties such as high wear resistance, low thermal expansion and high specific strength [1−4]. The cheap and easily available ceramic particles are SiC and Al_2O_3 which have been broadly used as reinforcements over a long period since the advent of AMCs. The progression of production techniques made it possible to prepare AMCs reinforced with several kinds of potential ceramic particles such as SiO_2 [5], TiO_2 [6], AlN [7], TiN [8], Si_3N_4 [9], TiC [10], B_4C [11], TiB_2 [12] and ZrB_2 [13].

AMCs are presently manufactured using a variety of established methods as well as specific patented methods. Powder metallurgy [14], mechanical alloying [15], stir casting [16], squeeze casting [17], compo casting [18] and spray deposition [19] are the conventional methods used to prepare AMCs. The mechanical behavior of the AMCs predominantly depends on production method used. The major factors which influence the mechanical behavior of AMCs are nature of distribution of ceramic particles in the aluminum matrix and the interfacial bonding [20]. All production methods are grouped into two categories which are known as solid state processing and liquid state processing. Each production method has its own constraints to prepare AMCs with certain combinations of matrix alloy and ceramic particles only. Consequently, lots of research emphases are being paid to develop the production methods to prepare AMCs. Although solid state processing provides desirable mechanical properties, the investment cost is high and unsuitable for mass production [21,22]. Liquid state

Corresponding author: J. DAVID RAJA SELVAM; E-mail: jdavidselvam@gmail.com
DOI: 10.1016/S1003-6326(16)64255-3

processing is preferred to producing AMCs because of its simplicity, facile adaptability and applicability to mass production [23]. Two routes are employed to produce AMCs through liquid state processing either by introducing ceramic particles externally to the aluminum melt or generating ceramic particles within the melt itself. External particle incorporation is called as ex situ fabrication and the internal particle generation is known as in situ fabrication. The challenges in ex situ fabrication are poor wettability between the molten aluminum and the ceramic particle, setting of ceramic particles at the bottom of the casting, formation of particle clusters, undesirable interfacial reactions and decomposition of ceramic particles [24,25]. In situ fabrication involves exothermal reactions between elements or between elements and compounds with molten aluminum to generate ceramic particles. In situ method exhibits several advantages over ex situ methods such as fine particle size, clean interface, good wettability between the reinforcement particles with the aluminum matrix and homogeneous distribution. Therefore, in situ method drew the attention of researchers in the past decade [26−28].

Some studies on aluminum alloy reinforced with in situ formed TiC particles were reported in the literatures [29−39]. TONG [29] developed Al/TiC AMCs by the in situ reaction between titanium and graphite powders at 1623 K and studied the microstructure. KERTI [30] produced Al/TiC AMCs by the in situ reaction between Al+Ti master alloy and elemental carbon at 1473 K. TYAGI [31] fabricated Al/TiC AMCs by the in situ reaction between titanium and silicon carbide powders at 1473 K and evaluated the tribological behavior. SHEIBANI and NAJAFABADI [32] assessed the possibility to produce Al/TiC AMCs by the in situ reaction between titanium dioxide and graphite powders at 1073 K. BIROL [33] estimated the effect of reaction temperature on the formation of Al/TiC AMCs by the in situ reaction between inorganic salt K_2TiF_6 and graphite powders. JI et al [34] investigated the creep behaviour of AA2618/TiC AMCs prepared by the in situ reaction between titanium and graphite powders at 1123 K. BAURI [35] investigated the effect of casting temperature and the ratio between titanium and carbon on microstructure of Al/TiC AMCs formed by the in situ reaction between titanium and graphite powder. LIANG et al [36] synthezised Al−4.5Cu/TiC by the in situ reaction between titanium and graphite powders at 1273 K and examined the microstructure. YIGEZU et al [37] reported the abrasive sliding wear behavior of Al–12%Si/TiC AMCs produced by the in situ reaction between titanium powder and activated charcoal at 1473 K. CHO et al [38] suggested that the addition of CuO reduces the reaction temperature required to form TiC particles by the in situ reaction between titanium and graphite powders. BASKARAN et al [39] analyzed the dry sliding wear behavior of AA7075/TiC AMCs developed by the in situ reaction between inorganic salt K_2TiF_6 and graphite powders at 1173 K.

In this work, an attempt is made to fabricate aluminum alloy AA6061 reinforced with TiC particles by the in situ reaction of inorganic salt K_2TiF_6 and ceramic powder SiC at elevated temperature with molten aluminum and study the effect of in situ formed TiC particles on microstructure and mechanical properties.

2 Experimental

AA6061 rods were kept inside a coated graphite crucible and were heated in an electrical furnace. The chemical composition of AA6061 aluminum alloy used in this study is given in Table 1. The inner wall of the crucible applied a coating to avoid contamination. The measured quantities of inorganic salt potassium fluotitanate (K_2TiF_6) and preheated ceramic powder SiC as presented in Table 2 were incorporated into the molten aluminum to form TiC particulates. The temperature of the molten aluminum was maintained at 1473 K. The melt was stirred intermittently for 60 min. The furnace provided an argon rich environment to prevent oxide formation at elevated casting temperature. The composite melt was transferred into a preheated die following the removal of slag. Castings were made with various amounts of TiC particles (0, 2.5% and 5%).

Table 1 Chemical composition of AA6061 aluminum alloy (mass fraction, %)

Mg	Si	Fe	Mn	Cu	Cr	Zn	Ni	Ti	Al
0.95	0.54	0.22	0.13	0.17	0.09	0.08	0.02	0.01	Bal.

Table 2 Calculated masses of chemicals

w(TiC)/%	m(K_2TiF_6)/g	m(SiC)/g
0	0	0
2.5	35	6
5	70	12

Specimens of required size were machined from the castings to carry out microstructure and mechanical characterization. Those specimens were polished according to standard metallographic technique and etched with Keller's reagent. The etched specimens were observed using scanning electron microscope (SEM), field emission scanning electron microscope (FESEM) and electron backscatter diffraction (EBSD). The metallographically polished samples were electro polished in a mixture of perchloric acid and methanol for EBSD studies. EBSD was carried out in an FEI Quanta

FEG SEM equipped with TSL-OIM software. Selected specimens were observed using transmission electron microscope (TEM). X-ray diffraction patterns (XRD) were recorded using Panalytical X-ray diffractometer. The microhardness was measured using a microhardness tester at 500 g load applied for 15 s. The tensile specimens were prepared as per ASTM E8M−04 standard having a gauge length of 40 mm, a gauge width of 7 mm and a thickness of 6 mm. Six such tensile specimens (two at top, two at middle and two at bottom) were prepared from each casting. The ultimate tensile strength (UTS) was estimated using a computerized universal testing machine. The fracture surfaces of the failed tensile specimens were observed using SEM.

3 Results and discussion

3.1 X-ray diffraction analysis of AA6061/TiC AMCs

Aluminum alloy AA6061 reinforced with TiC particulate AMCs was successfully synthesized by the in situ reaction of inorganic K_2TiF_6 and ceramic powder SiC to molten aluminum. The XRD patterns of the cast composites are presented in Fig. 1. The diffraction peaks of TiC particles are obviously visible and the intensities of the peaks increase as TiC content is increased. The in situ reactions as furnished in the subsequent equations result in the formation of TiC particles. It is also noticed in Fig. 1 that the peaks of aluminum in the AMCs are marginally shifted to higher 2θ compared to that of aluminum matrix owing to the formation of TiC particulate phase in the aluminum matrix.

$$3K_2TiF_6+13Al\longrightarrow 3Al_3Ti+4AlF_3+6KF \quad (1)$$

$$SiC+Al\longrightarrow Al_4C_3+Si \quad (2)$$

$$3Al_3Ti+Al_4C_3\longrightarrow 3TiC+13Al \quad (3)$$

The sequence of TiC formation can be summarized as follows. A detailed thermodynamic of in situ TiC formation is available elsewhere [26].

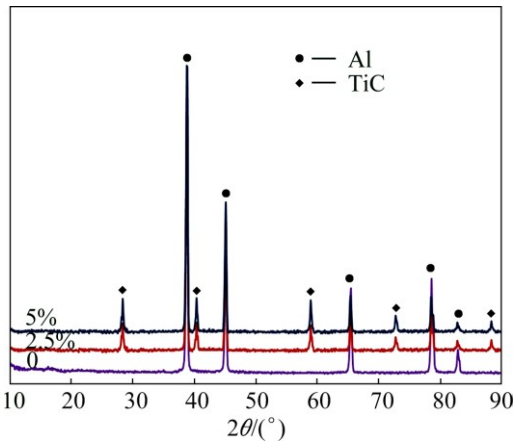

Fig. 1 XRD patterns of AA6061/TiC in situ composites

1) K_2TiF_6 and SiC respectively release Ti and C atoms in the melt. SiC is highly active at the elevated casting temperature and begins to decompose. The released Si helps to improve the castability of the aluminum composite. 2) Ti and C atoms combine with the molten aluminum and create intermetallic compounds namely Al_3Ti and Al_4C_3 respectively which act as source for Ti and B atoms. 3) Carbon atoms move towards Al_3Ti particles due to their high affinity towards Ti. 4) Reaction occurs between Ti and C atoms in a gap from Al_3Ti surface to form TiC. 5) Due to smaller size, carbon atoms start diffusing through TiC particles. 6) Dissolution of Al_3Ti particles due to natural cracking and disintegration of Al_3Ti particles which direct to increased rate of TiC formation. 7) Formation of TiC particles after complete reaction.

It is apparent from Fig. 1 that there is no trace of Al_3Ti or Al_4C_3 which confirms that the reaction is complete. Adequate holding time and appropriate mole ratio of inorganic salt and ceramic powder are required for complete reaction [26]. Though the furnace temperature was set to 1200 °C, the local melt temperature increased above 1250 °C because of the exothermic nature of the in situ reaction. SiC was added slightly in excess of the theoretical mole ratio to avoid the existence Al_3Ti phase. Lack of carbon atoms will make reaction (3) incomplete, leaving brittle Al_3Ti in the AMC. Absence of Al_3Ti peaks in Fig. 1 further indicates that the in situ formed TiC particles are thermodynamically stable and in equilibrium with molten aluminum. The in situ formed TiC particles do not decompose to produce any other compounds. The interface between the aluminum matrix and TiC particles tends to be free when no other compounds are present.

3.2 Microstructure of AA6061/TiC AMCs

The scanning electron micrographs of the prepared AA6061/TiC AMCs having various contents of TiC particles are shown in Fig. 2. Figure 2(a) depicts the micrograph of as-cast aluminum alloy AA6061. The microstructure consists of typical dendritic structure induced by solidification. Dendritic structure is formed due to faster cooling of the molten aluminum known as super cooling. The dendritic structure demonstrates elongated primary α(Al) dendritic arms which were estimated to have a higher aspect ratio. The average spacing between dendritic arms is computed to be 20−30 μm. The intermetallic phase Mg_2Si is observed around dendrites in Fig. 2. The formation can be explained using the binary phase equilibrium diagram of Al−Mg_2Si system shown in Fig. 3. The magnesium and silicon in this aluminum alloy combine to form Mg_2Si. The amount of Mg_2Si was calculated using the chemical composition provided in Table 1 and was estimated to be

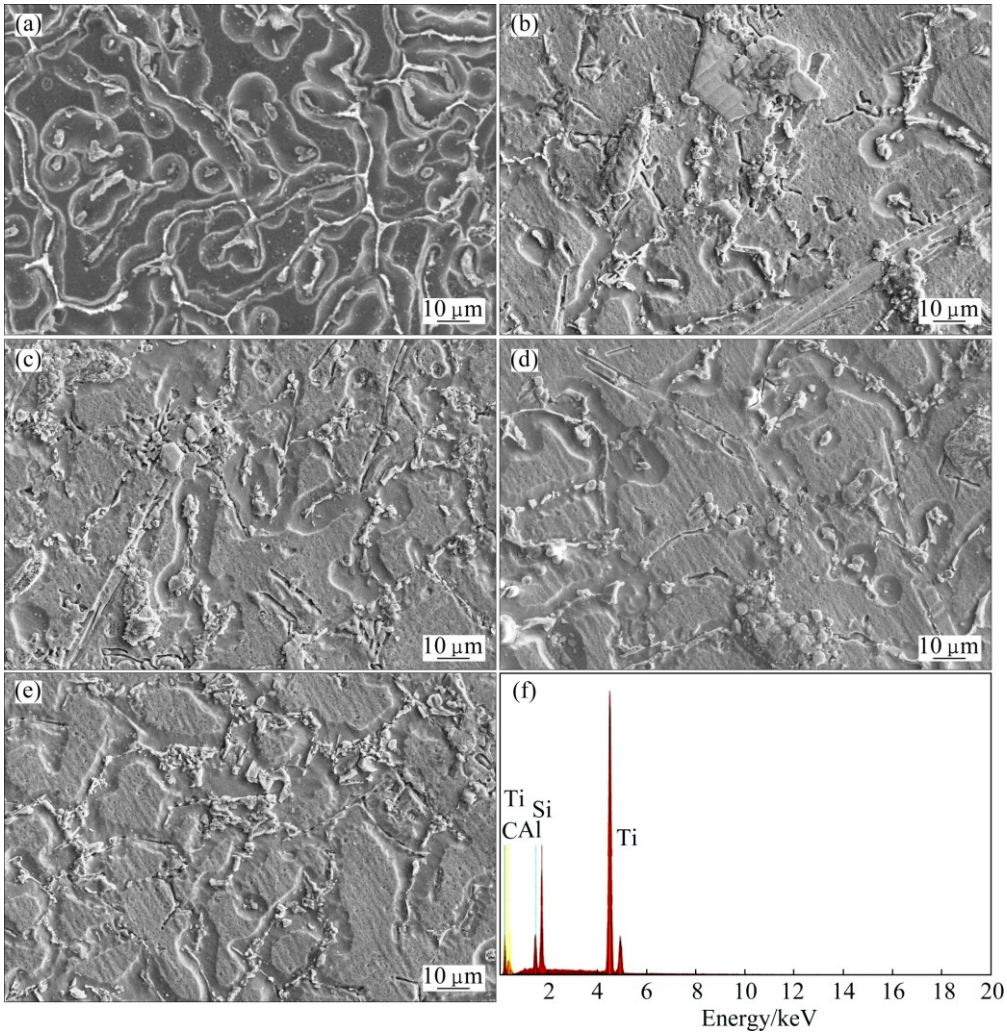

Fig. 2 SEM images of AA6061/TiC in situ composites at lower magnification containing TiC: (a) 0; (b, c) 2.5%; (d, e) 5%; (f) EDAX of 5% TiC

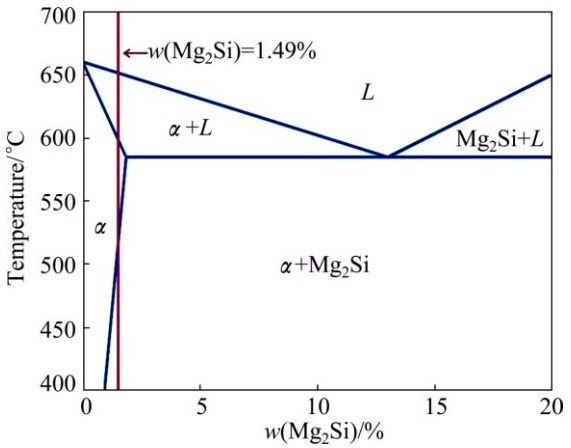

Fig. 3 Binary phase equilibrium diagram of Al−Mg_2Si system

1.49%. The Mg_2Si percentage of the AA6061 used in this work is marked as a vertical line in Fig. 3. The amount of Mg_2Si is higher than the solubility limit which solidifies through two-phase region. Hence, Mg_2Si phase is formed.

Figure 2(b) reveals the microstructure of AA6061/2.5% TiC AMCs. The dendritic structure is not present which confirms the formation of grainy structure. The composites were observed using EBSD to expose the grainy structure. The EBSD maps of AA6061/TiC AMCs having various contents of TiC particles are depicted in Figs. 4(a)−(c). The effect of TiC content on the average grain size of AA6061/TiC AMCs is furnished in Fig. 4(d). The EBSD maps exhibit a clear grainy structure in the composite (Figs. 4(b) and (c)). The EBSD maps confirm that the in situ formed TiC particles act as effective grain refiner and refine the grains of cast aluminum matrix [40]. The grain size reduces with an increase in TiC content (Fig. 4(d)). The in situ formed TiC particles completely change the dendritic structure of as-cast AA6061. The grain refinement can be ascribed to the following two factors. The presence of distributed TiC particles in the molten aluminum offers resistance to the growing α(Al) grains during the solidification process. TiC particles act as grain nucleation sites on

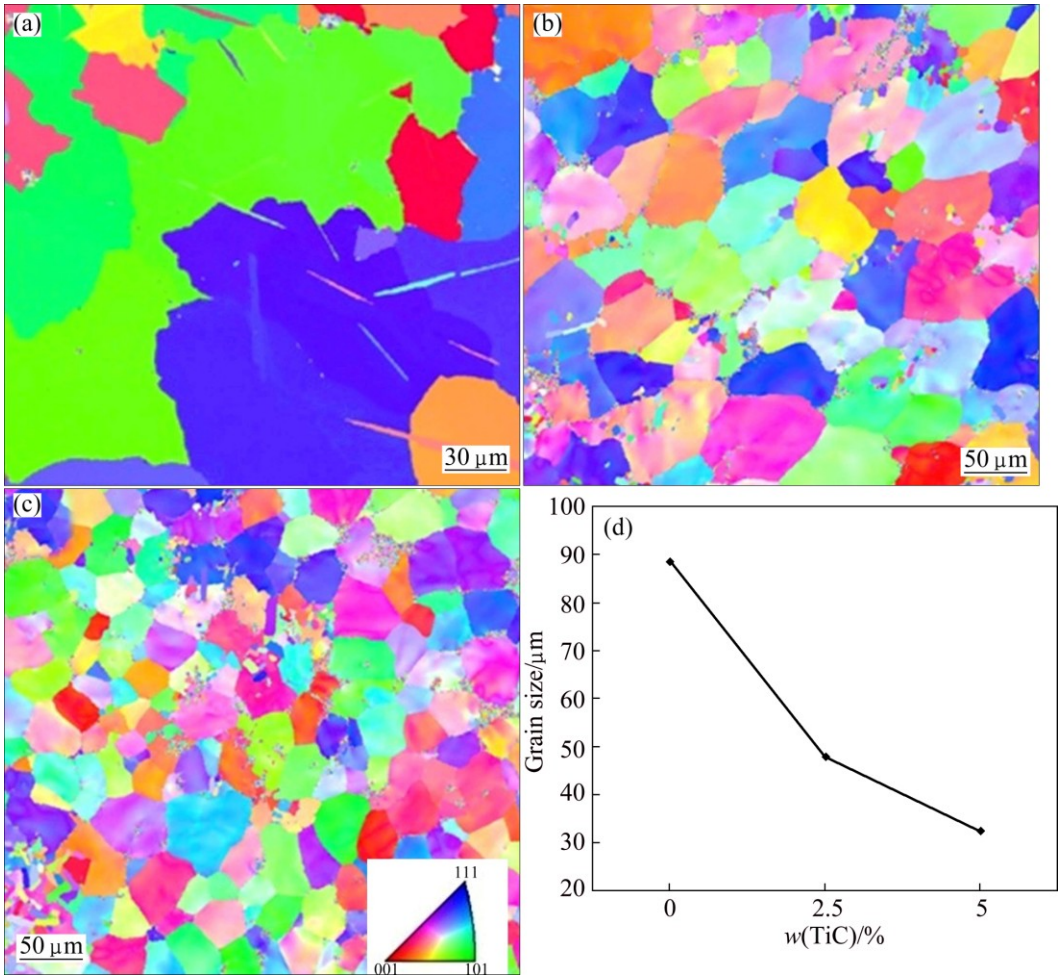

Fig. 4 EBSD (IPF + grain boundary) maps of AA6061/TiC in situ composites containing TiC: (a) 0; (b) 2.5%; (c) 5%; (d) Effect of TiC content on grain size of composites

which the aluminum grains proceed to solidify. The constitutional under cooling in front of the TiC particles leads them to act as grain nucleation sites. The overall microstructure consists of islands of α(Al) grains enclosed by hard TiC particle regions. The number TiC particles increases as the content of TiC in the composite is increased. This provides more grain nucleation sites which produce more resistance to the growth of α(Al) grains in the melt. As a result, the grain size decreases as the content of TiC is increased.

Figures 2(b)−(e) reveal that most of the in situ formed TiC particles are situated in intergranular regions. Fewer particles are observed inside grain boundaries. The micrographs are analyzed using image processing software and 75% of particles are located near intergranular regions. The nature of distribution of second phase particles in the molten aluminum is controlled by multiple factors including convection current in the melt, movement of the solidification front against the particles and buoyant motion of particles [41]. The velocity of the solidification front finally determines the particle distribution to be either intra or inter granular. Particles are either pushed or engulfed by the solidification front depending upon its velocity. If the velocity exceeds a critical value, the particles are surrounded by solidification front, leading to intra granular distribution and vice versa. The particle size and the temperature gradient influence the value of critical velocity. The intergranular distribution of TiC particles shows that the fine TiC particles are pushed by the solidification front.

The familiar casting defects such as porosity, shrinkages or slag inclusion are absent in the micrographs in Fig. 3, which demonstrates the quality of castings. Although the TiC particles are situated in intergranular regions, the overall distribution is considered to be homogenous. Particle free regions are scarce in the micrographs. A homogenous distribution of second phase particles in the aluminum matrix provides superior mechanical properties. The distribution of TiC particles is a function of the solidification process. The difference in density between the TiC particle and the

aluminum matrix plays critical part during solidification. Depending upon the magnitude of the density gradient, the ceramic particle will start to either sink or float. The suspension of ceramic particles in the aluminum melt for a longer duration is desirable to achieve homogenous distribution. The in situ method produces ceramic particles of very fine size. The average size of in situ formed TiC particle is measured to be less than 3 μm. The fine size is a result of high nucleation rate of in situ particles. HASHIM et al [42] reported that particles of size less than 10 μm will suspend in the aluminum melt for a long time and are least influenced by gravity. The fine size particles remain in suspension for a longer duration in the aluminum melt without settling at the bottom of the crucible. The sinking rate is insignificant. As TiC particles are formed by the in situ reaction, the molten aluminum spreads on the surface of the TiC particle in order to wet it. This wetting action retards the free movement of TiC particle within the melt. Thus, a homogeneous distribution is achieved. The EDAX analysis of AA6061/5%TiC AMC is given in Fig. 3 which identifies that the particles formed are TiC particles.

Figure 5 displays the micrographs of AA6061/TiC AMCs at higher magnification. The shape of the in situ formed TiC particles is manifested in Figs. 5(a) and (b). TiC particles exhibit various shapes like hexagonal, cubic and spherical. Some investigators noticed the shape of TiC particles to be hexagonal [36] while others reported spherical and cubic structure [33,34,38,39]. The shape of the in situ formed particles is affected by the growth kinetics prevailing within the melt. The crystalline shape is determined by the relative growth rate on the different planes. The presence of impurities in the aluminum melt induces high density of planar defects within the TiC grains. Those planar defects significantly influence the structure of TiC and promote the formation of TiC hexagonal platelet [43]. There are no blocky or needle shaped particles seen in Fig. 5. This substantiates the absence of Al_3Ti particles in the composite. The holding time is sufficient to complete the in situ reaction. It is further evident from Figs. 5(a) and (b) that a clear interface exists between the TiC particle and the aluminum matrix. TiC particles are not surrounded by any reaction products. The clear interface is attributed to the thermodynamic stability of the TiC particles. There is no interfacial reaction between aluminum matrix and TiC. Ex situ fabrication methods are susceptible to interfacial reaction due to thermodynamically instability of particles [24]. A clear interface is a prerequisite to increase the load bearing capacity of AMCs. There are no pores observed around TiC particles. The formation of TiC particles within the melt avoids external moisture carry-over and limits the creation of pores. Thus, it can be stated that the TiC particles are well bonded with the aluminum matrix. It is difficult to achieve good bonding due to the poor wettability of TiC particles. But, the increase in local melt temperature overcomes the poor wettability and causes good bonding.

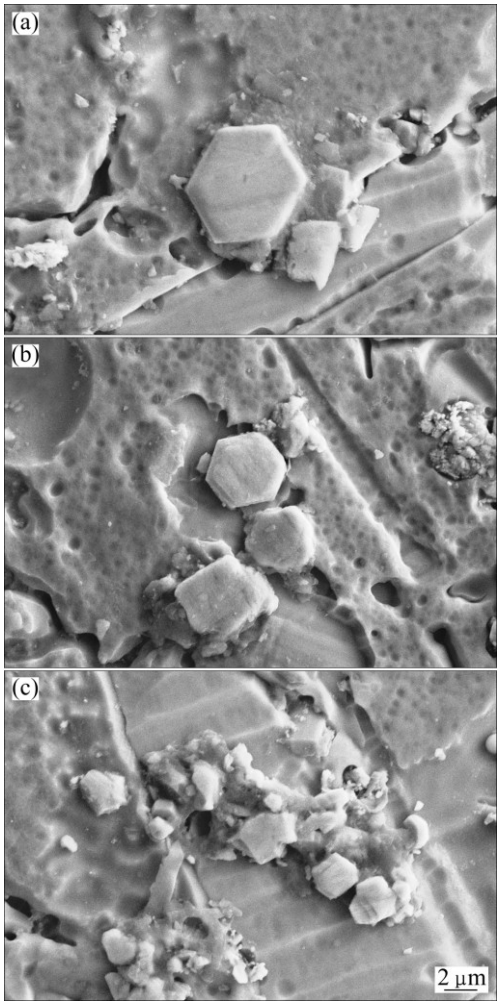

Fig. 5 SEM images of AA6061/TiC in situ composites at higher magnification containing TiC: (a) 2.5%; (b, c) 5%

The micrographs in Figs. 2(b)−(e) as discussed earlier are composed of homogenously distributed single TiC particles as well as TiC clusters. Figure 5(c) represents a magnified view of a single cluster. Similar clusters were also reported by other investigators [30,35,37,39]. The particles size in the cluster ranges from sub micron level to nano level. The mechanical response of clusters formed in the in situ reaction is contrary to the clusters present in ex situ composites [44]. Clusters of particles are formed in ex situ methods due to many factors such as poor wettability, inadequate stirring and density gradient between the aluminum matrix and the ceramic particle and drop in local melt temperature upon feeding of particles to the aluminum melt. The bonding between particles in such clusters is weak and acts as crack nucleation sites upon tensile

loading. But the particles in clusters formed by in situ reaction demonstrate good bonding. The exothermal in situ reaction creates good bonding between particles in clusters.

The TEM image of AA6061/5% TiC AMC is shown in Fig. 6. It confirms the existence of clear interface between the particle and the matrix. Strain fields are clearly visible around the particle. The aluminum alloy AA6061 and reinforcement TiC particles have dissimilar thermal expansion coefficients. The average thermal expansion coefficient of AA6061 is 2.4×10^{-5}/°C while that of TiC is 7.4×10^{-6}/°C. This variation in thermal expansion between aluminum matrix and TiC reinforcement creates strain fields around TiC particles during solidification. Each strain field consists of numerous dislocations appended to it.

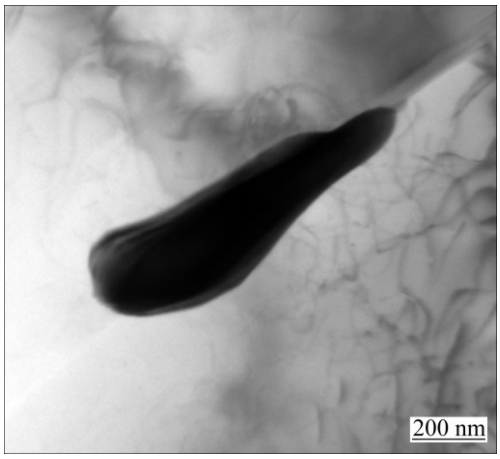

Fig. 6 TEM image of AA6061/5%TiC in situ composite showing clear interface and dislocation density

3.3 Mechanical properties of AA6061/TiC AMCs

The influence of in situ formed TiC particulate content on microhardness and UTS is depicted in Figs. 7(a) and (b), respectively. In situ formed TiC particles remarkably improve the microhardness and UTS of AA6061/TiC AMCs. AA6061/5%TiC AMC exhibits 83% higher microhardness and 21% higher UTS compared to unreinforced AA6061 alloy. The strengthening of AA6061 by in situ formed TiC particles can be expounded as follows. The interaction between TiC particles and dislocations retards the propagation of cracks during tensile loading. The in situ formed TiC particles are defect-free which retain their integrity during tensile loading. The grain refinement caused by the in situ TiC particles increases the area to resist the tensile load and strengthens the composite according to well known Hall−Patch relationship. The homogeneous distribution of TiC particles invokes Orowan strengthening mechanism [45]. The motion of dislocations is restricted by the homogeneous distribution and causes the dislocations to bow around

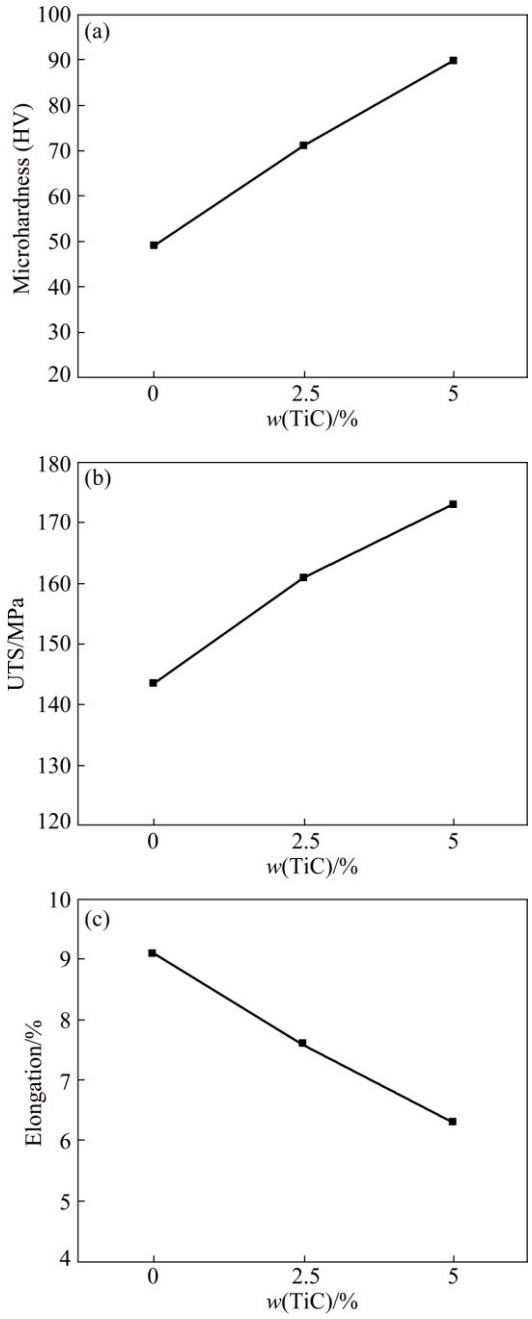

Fig. 7 Effect of TiC content on microhardness (a), tensile strength (b) and elongation (c) of AA6061/TiC in situ composites

the particles. Thus, Orowon loops are created around TiC particles which impede the progress of dislocations. The clear interface and good interfacial bonding delay the detachment of TiC particles from the aluminum matrix. Therefore, the microhardness and UTS of AMC are improved by TiC particles. The net effect by aforementioned factors increases as the content of TiC particles increases, which further raises the values of microhardness and UTS. The elongation of the AMCs drops against the content of TiC particles as presented in Fig. 7(c). Similar findings were reported by

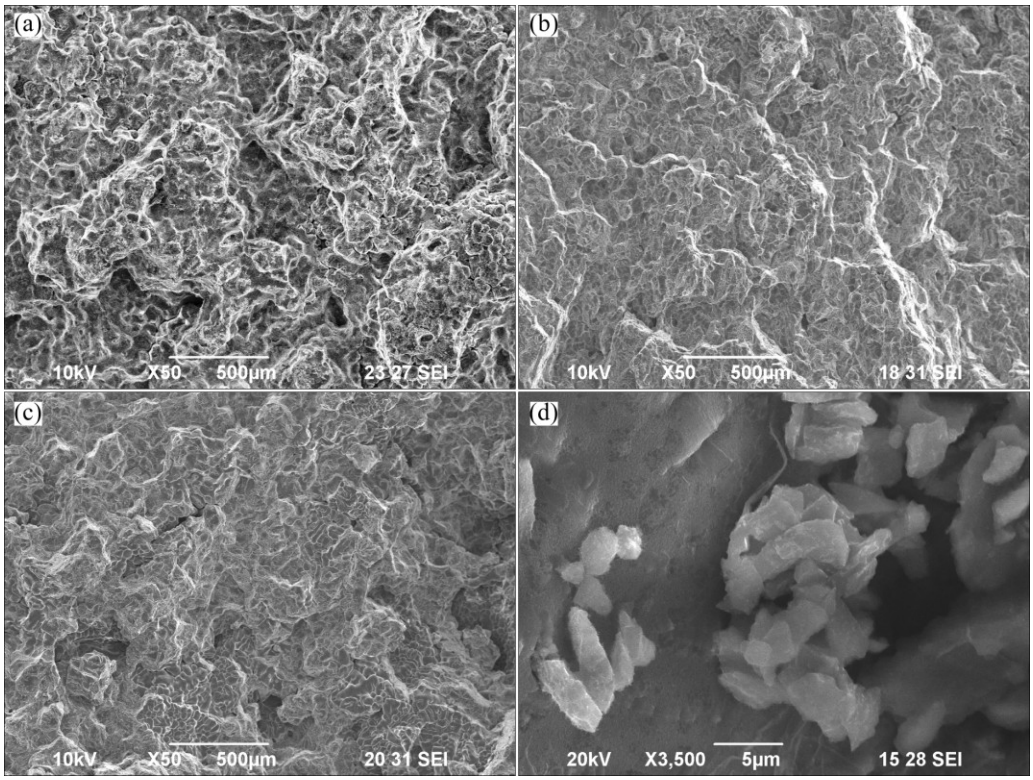

Fig. 8 Fracture morphologies of AA6061/TiC in situ composites containing TiC: (a) 0; (b) 2.5%; (c, d) 5%

LIANG et al [36]. The grain refinement and reduction of ductile matrix content reduces the ductility of the AMCs.

The fracture morphologies of the tensile tested specimens of AA6061/TiC are shown in Fig. 8. The fracture morphology of the matrix alloy AA6061 in Fig. 8(a) reveals large and uniformly distributed voids which point to ductile fracture. The fracture morphologies of the synthesized AA6061/TiC AMCs (Figs. 8(b) and (c)) present smaller size voids compared to that of aluminum, which indicate macroscopically brittle fracture and microscopically ductile fracture. The in situ formed TiC particles refine the grain size of aluminum alloy and diminish the ductility, which cause smaller size voids. The ductile shear band in the fracture morphology is a sign that some amounts of ductility is retained by the AMC. The magnified view of the fracture morphology of AA6061/5%TiC AMC is shown in Fig. 8(d). Fractured TiC particles stay intact in a number of places which give confirmation to the existence of good bonding between the aluminum matrix and in situ formed TiC particles.

4 Conclusions

AA6061/TiC AMCs were effectively produced by the in situ reaction of inorganic salt K_2TiF_6 and SiC with molten aluminum. The in situ reaction led to the formation of fine TiC particles. Possible intermetallic compounds including Al_3Ti and Al_4C_3 were detected in significant quantity in the AMCs. The majority of in situ formed TiC particles were located in inter granular regions. TiC particles acted as grain nucleation regions and refined the grains of aluminum matrix effectively. The microstructures of the produced AMCs revealed a homogeneous distribution of TiC particles having clear interface and good bonding. The in situ formed TiC particles displayed various shapes such as cubic, spherical and hexagonal. The mechanical properties of the AMCs enhanced as the content of TiC particles was increased.

Acknowledgement

The authors are grateful to Centre for Research in Metallurgy, Karunya University, FESEM Lab, Coimbatore Institute of Technology and OIM and Texture Lab, Indian Institute of Technology Bombay for providing the facilities to carry out this research work.

References

[1] SIVANANTH V, VIJAYARANGAN S, RAJAMANICKAM N. Evaluation of fatigue and impact behavior of titanium carbide reinforced metal matrix composites [J]. Materials Science and Engineering A, 2014, 597: 304−313.

[2] NI D R, WANG J J, ZHOU Z N, MA Z Y. Fabrication and mechanical properties of bulk NiTip/Al composites prepared by

friction stir processing [J]. Journal of Alloys and Compounds, 2014, 586: 368−374.

[3] AKBARI M K, BAHARVANDI H R, SHIRVANIMOGHADDAM K. Tensile and fracture behavior of nano/micro TiB_2 particle reinforced casting A356 aluminum alloy composites [J]. Materials and Design, 2015, 66: 150−161.

[4] CHEN H S, WANG W X, LI Y L, ZHANG P, NIE H H, WU Q C. The design, microstructure and tensile properties of B_4C particulate reinforced 6061Al neutron absorber composites [J]. Journal of Alloys and Compounds, 2015, 632: 23−29.

[5] HEMANTH J. Abrasive and slurry wear behavior of chilled aluminum alloy (A356) reinforced with fused silica (SiO_{2p}) metal matrix composites [J]. Composites: Part B, 2011, 42: 1826−1833.

[6] RAMESH C S, ANWAR KHAN A R, RAVIKUMAR N, SAVANPRABHU P. Prediction of wear coefficient of Al6061−TiO_2 composites [J]. Wear, 2005, 259: 602−608.

[7] ASHOK KUMAR B, MURUGAN N. Metallurgical and mechanical characterization of stir cast AA6061-T6−AlN_p composite [J]. Materials and Design, 2012, 40: 52−58.

[8] HASHEMI R, HUSSAIN G. Wear performance of Al/TiN dispersion strengthened surface composite produced through friction stir process: A comparison of tool geometries and number of passes [J]. Wear, 2015, 324−325: 45−54.

[9] RAMESH C S, KESHAVAMURTHY R. Slurry erosive wear behavior of Ni−P coated Si_3N_4 reinforced Al6061 composites [J]. Materials and Design, 2011, 32: 1833−1843.

[10] GOPALAKRISHNAN S, MURUGAN N. Production and wear characterisation of AA 6061 matrix titanium carbide particulate reinforced composite by enhanced stir casting method [J]. Composites: Part B, 2012, 43: 302−308.

[11] KALAISELVAN K, DINAHARAN I, MURUGAN N. Characterization of friction stir welded boron carbide particulate reinforced AA6061 aluminum alloy stir cast composite [J]. Materials and Design, 2014, 55: 176−182.

[12] ZHANG S L, YANG J, ZHANG B R, ZHAO Y T, CHEN G, SHI X X, LIANG Z P. A novel fabrication technology of in situ TiB_2/6063Al composites: High energy ball milling and melt in situ reaction [J]. Journal of Alloys and Compounds, 2015, 639: 215−223.

[13] TIAN K, ZHAO Y, JIAO L, ZHANG S, ZHANG Z, WU X. Effects of in situ generated ZrB_2 nano-particles on microstructure and tensile properties of 2024Al matrix composites [J]. Journal of Alloys and Compounds, 2014, 594: 1−6.

[14] ABDIZADEH H, EBRAHIMIFARD R, BAGHCHESARA M A. Investigation of microstructure and mechanical properties of nano MgO reinforced Al composites manufactured by stir casting and powdermetallurgy methods: A comparative study [J]. Composites: Part B, 2014, 56: 217−221.

[15] NIE C, GU J, LIU J, ZHANG D. Investigation on microstructures and interface character of B_4C particles reinforced 2024Al matrix composites fabricated by mechanical alloying [J]. Journal of Alloys and Compounds, 2008, 454: 118−122.

[16] YARA A A, MONTAZERIAN M, ABDIZADEH H, BAHARVANDI H R. Microstructure and mechanical properties of aluminum alloy matrix composite reinforced with nano-particle MgO [J]. Journal of Alloys and Compounds, 2009, 484: 400−404.

[17] XIU Z, YANG W, CHEN G, JIANG L, MAC K, WU G. Microstructure and tensile properties of Si_3N_{4p}/2024Al composite fabricated by pressure infiltration method [J]. Materials and Design, 2012, 33: 350−355.

[18] ZHANG L J, QIU F, WANG J G, JIANG Q C. High strength and good ductility at elevated temperature of nano-SiC_p/Al2014 composites fabricated by semi-solid stir casting combined with hot extrusion [J]. Materials Science and Engineering A, 2015, 626: 338−341.

[19] SRIVASTAVA V C, OJHA S N. Microstructure and electrical conductivity of Al−SiC_p composites produced by spray forming process [J]. Bulletin of Materials Science, 2005, 28: 125−130.

[20] MIRACLE D B. Metal matrix composites–From science to technological significance [J]. Composites Science and Technology, 2005, 65: 2526−2540.

[21] TORRALBA J M, DA COSTA C E, VELASCO F. P/M aluminum matrix composites: An overview [J]. Journal of Materials Processing Technology, 2003, 133: 203−206.

[22] SURYANARAYANA C, AL-AQEELI N. Mechanically alloyed nanocomposites [J]. Progress in Materials Science, 2013, 58: 383−502.

[23] TAHA M A. Practicalization of cast metal matrix composites (MMCCs) [J]. Materials and Design, 2001, 22: 431−441.

[24] YIGEZU B S, JHA P K, MAHAPATRA M M. The key attributes of synthesizing ceramic particulate reinforced Al-based matrix composites through stir casting process: A review [J]. Materials and Manufacturing Processes, 2013, 28: 969−979.

[25] HASHIM J, LOONEY L, HASHMI M S J. Metal matrix composites: Production by the stir casting method [J]. Journal of Materials Processing Technology, 1999, 92−93: 1−7.

[26] TJONG S C, MA Z Y. Microstructural and mechanical characteristics of in situ metal matrix composites [J]. Materials Science and Engineering R, 2000, 29: 49−113.

[27] PRAMOD S L, BAKSHI S R, MURTY B S. Aluminum-based cast in situ composites: A review [J]. Journal of Materials Engineering and Performance, 2015, 24: 2185−2207.

[28] CHEN F, CHEN Z, MAO F, WANG T, CAO Z. TiB_2 reinforced aluminum based insitu composites fabricated by stir casting [J]. Materials Science and Engineering A, 2015, 625: 357−368.

[29] TONG X C. Fabrication of in situ TiC reinforced aluminum matrix composites Part I Microstructural characterization [J]. Journal of Materials Science, 1998, 33: 5365−5374.

[30] KERTI I. Production of TiC reinforced-aluminum composites with the addition of elemental carbon [J]. Materials Letters, 2005, 59: 3795−3800.

[31] TYAGI R. Synthesis and tribological characterization of in situ cast Al−TiC composites [J]. Wear, 2005, 259: 569−576.

[32] SHEIBANI S, NAJAFABADI M F. In situ fabrication of Al−TiC metal matrix composites by reactive slag process [J]. Materials and Design, 2007, 28: 2373−2378.

[33] BIROL Y. In situ synthesis of Al−TiC_p composites by reacting K_2TiF_6 and particulate graphite in molten aluminium [J]. Journal of Alloys and Compounds, 2008, 454: 110−117.

[34] JI F, MA M Z, SONG A J, ZHANG W G, ZONG H T, LIANG S X, OSAMU Y, LIU R P. Creep behavior of in situ TiC_p/2618 aluminum matrix composite [J]. Materials Science and Engineering A, 2009, 506: 58−62.

[35] BAURI R. Synthesis of Al−TiC in-situ composites: Effect of processing temperature and Ti:C ratio [J]. Transactions of the Indian Institute of Metals, 2009, 62: 391−395.

[36] LIANG Y F, ZHOU J E, DONG S Q. Microstructure and tensile properties of in situ TiC_p/Al−4.5wt.% Cu composites obtained by direct reaction synthesis [J]. Materials Science and Engineering A, 2010, 527: 7955−7960.

[37] YIGEZU B S, JHA P K, MAHAPATRA M M. Effect of sliding distance, applied load, and weight percentage of reinforcement on the abrasive wear properties of in situ synthesized Al−12%Si/TiC composites [J]. Tribology Transactions, 2013, 56: 546−554.

[38] CHO Y H, LEE J M, KIM H J, KIM J J, KIM S H. Feasible process for producing in situ Al/TiC composites by combustion reaction in an Al melt [J]. Metals and Materials International, 2013, 19: 1109−1116.

[39] BASKARAN S, ANANDAKRISHNAN V, DURAISELVAM M. Investigations on dry sliding wear behavior of in situ casted

AA7075−TiC metal matrix composites by using Taguchi technique [J]. Materials and Design, 2014, 60: 184−192.
[40] VINOD KUMAR G S, MURTY B S, CHAKRABORTY M. Development of Al−Ti−C grain refiners and study of their grain refining efficiency on Al and Al−7Si alloy [J]. Journal of Alloys and Compounds, 2005, 396: 143−150.
[41] BAURI R, YADAV D, SUHAS G. Effect of friction stir processing (FSP) on microstructure and properties of Al−TiC in situ composite [J]. Materials Science and Engineering A, 2011, 528: 4732−4739.
[42] HASHIM J, LOONEY L, HASHMI M S J. Particle distribution in cast metal matrix composites—Part I [J]. Journal of Materials Processing Technology, 2002, 123: 251−257.
[43] LI S B, XIANG W H, ZHAI H X, ZHOU Y. Formation of TiC hexagonal platelets and their growth mechanism [J]. Powder Technology, 2008, 185: 49−53.
[44] MICHAEL RAJAN H B, RAMABALAN S, DINAHARAN I, VIJAY S J. Synthesis and characterization of in situ formed titanium diboride particulate reinforced AA7075 aluminum alloy cast composites [J]. Materials and Design, 2013, 44: 438−445.
[45] ZHANG Z, CHEN D L. Contribution of Orowan strengthening effect in particulate-reinforced metal matrix nano composites [J]. Materials Science and Engineering A, 2008, 483−484: 148−152.

碳化硅与氟钛酸钾原位反应制备 AA6061/TiC 铝基复合材料的显微组织与力学性能表征

K. JESHURUN LIJAY[1], J. DAVID RAJA SELVAM[2], I. DINAHARAN[3], S. J. VIJAY[2]

1. School of Mechanical Sciences, Karunya University, Coimbatore 641114, Tamil Nadu, India;
2. Center for Research in Metallurgy, School of Mechanical Sciences, Karunya University, Coimbatore 641114, Tamil Nadu, India;
3. Department of Mechanical Engineering Science, University of Johannesburg, Auckland Park Kingsway Campus, Johannesburg 2006, South Africa

摘　要：采用 K_2TiF_6 无机盐和 SiC 陶瓷颗粒与铝熔体原位反应制备不同含量 TiC 颗粒(0, 2.5%, 5%, 质量分数)增强 AA6061 铝合金。为分解 SiC 释放碳原子，合金在高温下进行铸造，并保温一段时间。X 射线衍射分析表明铝基复合材料中只生成 TiC 颗粒而未见其他金属间化合物。采用场发射扫描电子显微镜(FESEM)和背散射电子衍射(EBSD)分析 AA6061/TiC 复合材料的显微组织。结果表明原位生成的 TiC 颗粒分布均匀，界面清晰，结合良好，并具有立方、球形和六方等形状。EBSD 图像表明 TiC 颗粒对复合材料具有明显的晶粒细化效果。TiC 颗粒可提高铝基复合材料的显微硬度和抗拉强度。

关键词：铝基复合材料；碳化钛；背散射电子衍射；铸造；显微组织；力学性能

(Edited by Yun-bin HE)